ELSEVIER

Self-assembled monolayers of alkylsiloxanes on SrTiO₃ substrates

Boike L. Kropman*, Dave H. A. Blank and Horst Rogalla
Department of Applied Physics, University of Twente, 7500 AE Enschede, The Netherlands
(Received 11 March 1996; revised 5 July 1996)

The formation and structure of alkyltrichlorosilanes on several types of SrTiO₃ substrates have been studied. The silanes adsorb spontaneously from a hexadecane solution and form monolayers on all the substrates used. Characterization has been performed by atomic force microscopy, wettability, angle resolved X-ray photoelectron spectroscopy, reflection absorption infrared spectroscopy, and spectroscopic ellipsometry. It was found that highly ordered and densely packed monolayers were formed below a certain temperature. © 1997 Elsevier Science Ltd. All rights reserved.

(Keywords: self-assembly; SrTiO₃; alkyltrichlorosilanes)

INTRODUCTION

Self-assembled monolayers[1] (SAMs) have been investigated extensively during the past few years. Most attention has been directed towards the formation and the final structure of simple alkanethiols on gold. It was found that highly organized monolayers can be grown. During the spontaneous adsorption, the molecules bind to the substrate via a gold–sulfur bond, with tilted chains (~30°) to maximize the van der Waals interaction between neighbouring chains. A variety of tailgroups can be exposed to the surface, offering possibilities to selectively tailor surface properties such as, e.g., wettability, friction and optical response[1]. Despite all the progress made in the thiol system, increasing effort has been put to a more general class of SAMs: alkylsiloxanes on oxidic substrates such as SiO₂[1], but also mica[2a], ZnSe[2b] and AU[2c] have been investigated. The resulting films are more general because the substrate specific binding mechanism is absent, resulting in substrate-independent final structures.

In this study, strontium titanate (SrTiO₃, STO) has been investigated as an alternative substrate material for the growth of self-assembled monolayers. Perovskite materials, like STO, have found an increased interest due to a number of new applications in, for example, the growth of superconducting high critical temperature (HTc) materials[3a]. They possesse a high dielectric constant at room temperature, making them interesting for application in high storage capacitors. Furthermore, these substrates have been used as photocatalysts for the decomposition of H₂O. Similar materials, such as barium titanate and lead zirconate titanate, show ferroelectricity, piezoelectricity, etc.[3b]. A further attractive property of this substrate is that one can systematically vary the conductivity of the substrate by doping it with Nb (STO:Nb). The used Nb-doped crystal (doping level is 0.5wt%) is semi-conducting and permits imaging of its surface by STM.

SrTiO₃ is a crystal with the cubic perovskite ABO₃ structure. The cubic unit cell ($a = 3.9$ Å) contains layers of, alternately, SrO and TiO₂, stacked in the *c*-direction. The (001) surface, which is the most commonly used surface, is known to be terminated almost exclusively with either SrO or TiO₂. The (110) surface, on the other hand, possesses, alternately, rows of SrO and TiO₂ in the plane of the surface. Finally, the lesser-known STO(103) or (305) face is known to roughen considerably (long triangular and 5–10 nm high ridges are formed, with one of the facets made of the (101) plane) if annealed above 1050°C. This latter surface is used to test the influence of roughness of the substrate on the properties of the resulting monolayers.

EXPERIMENTAL

General

Octadecyltrichlorosilane (OTS, 95%), dodecanetrichlorosilane (DTS, 98%), *n*-hexadecane (HD, 99 + %), chloroform, acetone, ethanol, phosphoric acid (all p.a. quality) were obtained from Aldrich and used as received. SrTiO₃ substrates of different orientations were obtained from ESCETE, Enschede, The Netherlands. Some of the substrates were annealed before-

---

* To whom correspondence should be addressed
(e-mail: b.l.kropman@tn.utwente.nl)

hand at 1050°C (heating and cooling rate $\pm5°C\,min^{-1}$) for at least 20h. The substrates were further cleaned by sonicating in a sequence of solvents (chloroform, acetone, alcohol) several times and dipped in a diluted phosphoric acid (1:500 H_2O) solution for 1 min and placed in the silanating solution. For each adsorption, the solution was freshly prepared by solving 1 mM alkyltrichlorosilane (OTS or DTS) in hexadecane. The deposition parameters are controlled as well as possible, i.e. the adsorption takes place in an excicator to minimize the influence of environmental humidity (relative humidity is then reduced to 20–40%) and the temperature is controlled at $\sim20°C^4$. Adsorption times were kept between 2 and 12h, although no difference in film quality was found for these extremes. To remove physisorbed and/or complexed HD, the mono-layer was sonicated for several minutes in chloroform and ethanol.

Scanning probe microscopies (SPM)

A Digital Instruments Nanoscope IIIa was utilized to image the topography of the surface. Most of the images were made using the tapping mode of the atomic force microscope (AFM), but all results were confirmed by contact mode AFM and STM (for STO:Nb). Care was taken to avoid contact forces above several nanoNewtons (nN). Immediately after engagement of the cantilever, the contact force was minimized and amounted to less than 5 nN. If such forces were used in the contact mode, the topography exactly resembled that of the tapping mode images.

Wetting

Contact angle measurements were carried out on a home-built system. Drops of a fixed volume (5 μl) were placed at several places on the substrate. First, the sessile drop was captured by a CCD camera and recorded on a videorecorder. The volume of the drop was slowly increased, and the advancing angle was measured at the instant the drop started moving. This was done several times at several places on the sample to obtain some statistics. The same was done for decreasing volume of the drop (receding contact angle). Two different probe liquids

were used: water (H_2O), a polar liquid with high surface tension and *n*-hexadecane, a nonpolar liquid with low surface tension. The error in the measurement of the contact angle is estimated to be 1° for the water contact angles, and 0.5° for hexadecane, but sample-to-sample variations and variations on the sample itself are larger. Estimations (from the standard deviations) of these variations are shown in parentheses in *Table 1*.

ARXPS

A Kratos XSAM 800 spectrometer was used for angular resolved XPS measurements. The base pressure of the system is 4×10^{-10} Torr. Monochromatic X-rays are generated by a Mg source ($K_\alpha = 1254.6$ eV), directed towards the surface where the beam generates photoelectrons from the core levels (s, p), and detected by a hemispherical electron energy analyser. Pass energies used for survey scans are 50 eV, whereas for the high resolution scans 20 eV were used. The spectra were background-subtracted and fitted by a home-built computer program. All fits are made with 100% Gaussians. To determine the thickness of the mono-molecular film, spectra were not only taken at zero take off angle φ, but also at other angles (10, 20, 30, and 50° away from the surface normal).

RAIRS

Reflection absorption infrared spectroscopy (RAIRS) was performed on a BioRad FTS-60A spectrometer. An infrared lightsource, radiating continuously between 500–4000 cm^{-1}, is reflected at near grazing incidence (88° off the surface normal) and detected by an MCT detector. In general, the full spectral range is recorded with 4 cm^{-1} resolution and between 500 and 1000 scans are co-added and averaged to obtain a good signal-to-noise ratio. The spectrum of the reference substrate is recorded first and later subtracted from the derivatized sample. The sample stage compartment is purged by nitrogen to minimize the amount of H_2O from the sample compartment. Although the compartment is purged, some regions of interest were masked by the presence of traces of H_2O (especially between 1300 and 1500 cm^{-1}).

Table 1 Contact angles for different faces of STO[a,b,c]

	θ_a^{H2O}	θ_r^{H2O}	θ_a^{HD}	θ_r^{HD}	δ^{H2O}	δ^{HD}
OTS/STO(001)	116 (1.3)	103	41 (3.4)	38	0.21	0.02
OTS/STO(001)[d]	113 (1.4)	103	44 (4.4)	38	0.16	0.07
OTS/STO(110)	115 (1.5)	103	44 (1.4)	34	0.22	0.11
OTS/STO(103)	119 (2.2)	104	40 (1.6)	< 10	0.25	
OTS/STO:Nb(001)	114 (1.9)	103	41 (4.9)	33	0.16	0.09

[a] θ_a = advancing CA, θ_r = receding CA, H_2O = water, HD = *n*-hexadecane
[b] δ = hysteresis, defined as $\cos\theta_r - \cos\theta_a$
[c] Value between parentheses is estimation of error based on standard deviation
[d] Substrate annealed (at 1050°C) prior to adsorption

SE

Spectroscopic ellipsometry was performed on a home-built rotating polarizer ($P_{rot}SA$ at 67Hz) spectrometer. A Xe lightsource was used to produce a beam with 3mm diameter, ranging in energy from 1.5 to 4.5eV (850–250nm). The angle of incidence is set close to Brewster's angle for $SrTiO_3$ (~70°), where the ellipsometric parameters Δ and Ψ are most sensitive to changes. The system was designed for growth studies of sputter-deposited $YBa_2Cu_3O_\delta$, on $SrTiO_3$ substrates in UHV (base pressure p~10^{-7}Torr). To minimize the pollution of (especially unsilanized) samples, all samples were measured in a vacuum. The Fourier coefficients of the incident beam are measured and can be related to the more convenient ellipsometric parameters.

RESULTS AND DISCUSSION

Scanning probe microscopies (SPM)

The topography of the as-cleaned substrates is studied to correlate their roughness to the final monolayer structure. All substrates were atomically flat with RMS roughnesses less than 2Å. No steps could be observed, only a vague grain-like structure with some variations in height of 1.9Å. If STO(001) substrates were annealed at $T > 1050°C$ beforehand, steps appeared at regular distances. Since the step-heights are a single unit cell, 3.9Å, this is strongly indicative of a single terminating plane, in contrast to the as-cleaned substrates. Kawasaki found for $SrTiO_3$ that TiO_2 is the stable terminating plane[5].

The first experiments on self-assembly on all surfaces of STO were done in a normal laboratory environment (T~25°C, humidity~75%), resulting in films with reasonable wetting characteristics, but showing a high island density on the surface. As seen later, ellipsometry confirmed the formation of films with thicknesses d larger than 4nm. These 'islands' have a random shape and size. All islands have a discrete height of ~5.3nm high, indicating the formation of adventitious double layers, so-called lamellae, on top of a monomolecular film. Sometimes, even a second lamellar structure is formed on top of the first (the fourth and fifth layer of OTS). An example is shown in *Figures 1a* and *c*. Since only the first layer is chemisorbed onto the surface via the siloxane linkages, these extra lamellae are physisorbed onto the first layer. Although these lamellae are stable in the usual solvents (even ultrasonicated), they can be removed easily by rubbing with a paper tissue.

If a monolayer is adsorbed on the substrate and the adsorption conditions have been controlled carefully enough (T~20°C, humidity~20–40%), almost no texture can be seen on the surface, indicating homogeneous growth of the monomolecular layer; see

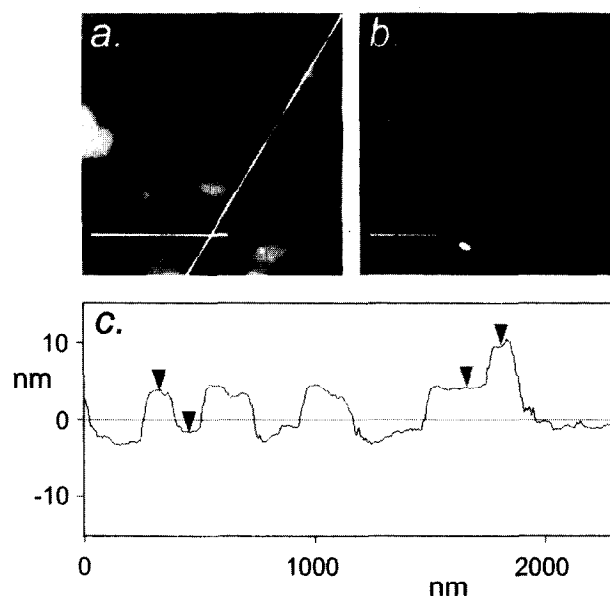**Figure 1** (a) 2×2μm AFM image (tapping mode) of the surface of OTS on SrTiO₃:Nb(001), showing lamellae with discrete (~5.3nm) heights (the marker has a length of 250nm); (b) 1×1μm AFM (contact mode) of the surface of an OTS monomolecular layer on SrTiO₃(001), with almost no islands (the marker has a length of 250nm); (c) line scan along the line shown in (a)

Figure 1b. Measurements on the thickness of the film by ellipsometry show that such films are approximately 2.2–2.4nm thick, confirming the growth of a single molecular layer.

Wettability

To check the cleaning procedure, as described in the experimental section, contact angles (CAs) were measured after each consecutive step in this procedure. Before cleaning, the CA of water is, depending on the 'history' of the substrate, approximately 70°. The solvent cleaning results in a decrease to approximately 43° whereas, upon the final phosphoric acid dip, the CA drops to $\leq$25°, rendering a hydrophilic (i.e. a hydroxylated) surface. If the substrate was immersed in pure n-hexadecane (HD) the CA again increases up to 45°. If monolayers are formed by immersion of the substrate in the 1mM solution of OTS in HD, the CA significantly increases to $>$110°.

In *Table 1*, the CA data have been summarized for monolayers of OTS on the four different substrates of STO used in this study. Typical values for the advancing water CA are 115$\pm$2°, whereas the HD CAs fall in the range 42$\pm$2°. Such CAs indicate the formation of a methyl-terminated surface[16]. Our results are comparable with data for the OTS monolayers on SiO_2[4,7,8], although the values for the HD CAs are somewhat smaller than observed for OTS/SiO₂. The observed hysteresis in the water CA is larger than for comparable thiols on gold[6] (δ~0.1–0.15), but it is known that for buried polar groups the observed hysteresis increases. Other reports for OTS

observe comparable hysteresis values[8] ($\delta \sim 0.2$–0.25). First attempts, however, at an adsorption temperature of $\sim 25°C$ resulted in comparable advancing CA, with much higher hysteresis ($\delta \sim 0.35$). The higher hysteresis is due to the formation of lamellae.

It was found that hexadecane (HD) provided a better means of determining the extent of ordering at the surface: better films gave significantly higher CAs, whereas the water CA was consistently high ($> 115°$). Measurements, performed in an early stage where the temperature during adsorption was not controlled at all, yielded lower quality films and low HD CAs ($\theta_a < 40°$). If, however, such a monolayer film was annealed at 150°C, the water CA did not change, but an increase in both the final film quality and the HD CA was found (θ_a from 36 to 43° and θ_r from 26 to 37°). Removal of HD molecules incorporated in the monolayer and lamellae on top of the monolayer can be responsible for such an increase. The HD CA is relatively low for a rough substrate as STO(103) and the receding CA even vanishes on this substrate.

ARXPS

The XPS survey scans were taken at a perpendicular take-off angle $\varphi = 0°$. The as-cleaned substrates only show the elements of $SrTiO_3$ plus a small and broad carbon contamination peak. The binding energy of the C 1s peak indicates 'pure' carbon. No Si is present on these substrates. If an OTS film is measured, the intensity (as measured by the peak intensity and area) of the Sr, Ti and O decreases dramatically, whereas the C 1s contribution increases significantly. Si appears in all spectra and a small Nb peak only in the STO:Nb spectra. Monolayer films with shorter chains and/or lower quality (as judged by RAIRS and SE) show a lower atomic concentration of C, and higher concentrations of elements from the substrate. The Si concentration, however, remains almost unchanged.

High resolution scans (summarized in *Table 2*) were taken at $\varphi = 0°$. They show the expected binding energies (BE) for the elements of $SrTiO_3$[9]. It is seen for all monolayer films that the C 1s peak becomes much narrower than for bare substrates. This is true for all monomolecular films measured (including films that show degraded properties, due to adsorption above $\sim 25°C$). Due to the adsorption, a Si 2p peak appears in the spectra at 102.5eV (see *Figure 2a*),

indicating the formation of Si_2O_3[10]. This is consistent with the formation of a siloxane network.

The oxygen region around 530eV is very interesting because it shows a complex envelope function. However, fitting of this envelope function is not very accurate. From the reference substrates (unsilanized STO), it is clear that more than one oxygen species is present on the surface: at first sight, two peaks are present. The sharp lower BE peak (at $\sim 530.1eV$) belongs to the titanate oxygen[9], whereas the broader high BE peak (at $\sim 531.4eV$) can be assigned to the oxygen in the hydroxylated topmost layer of the surface. This is confirmed by ARXPS: the titanate oxygen peak is decreased for higher take-off angles, whereas the hydroxyl oxygen peak increases, indicating its origin from the topmost layer (see *Figure 2b*). However, fitting with two peaks is not very satisfactory since it yields quite large uncertainties (as compared to the other peaks). The error decreases if a third oxygen species is introduced, but these results cannot be interpreted consistently. For the derivatized samples, the high BE peak is attributed to the formation of a siloxane network (binding to the substrate and neighbouring chains).

From the φ-dependent attenuation of the photoelectrons in an overlayer, one can determine the thickness of the overlayer[11], even in the case of a layered substrate. The decrease in intensity $I(\varphi)$ of elements from the substrate (e.g. the Sr 3d peak), as a function of take-off angle, can be related to the thickness of a homogeneous overlayer according to:

$$\ln\left(\frac{N(\varphi)}{G(\varphi)}\right) = \frac{d}{\lambda_{top}}\left(1 - \frac{1}{\cos\varphi}\right)$$

where $N(\varphi) = I(\varphi)/I(0)|_{top}$, $G(\varphi) = I(\varphi)/I(0)|_{sub}$, d is the thickness of the overlayer and λ_{top} is the attenuation length of photoelectrons at the kinetic energy KE ($= K_x - BE$) of the specific photoelectrons. The attenuation length can be interpolated from measurements by Laibinis *et al.*[12] for n-alkanethiols on Cu, Ag and Au. The calculations were performed for both Ti 2p and Sr 3d peaks; it was found that for good quality monolayers, as judged by the infrared measurements and AFM, the thicknesses determined by the attenuation of the Sr photoelectrons is in the range 2.2–2.5nm. For Ti 2p photoelectrons, much thinner films (~ 1.3–1.9nm) are found. The values found for Sr

Table 2 Results of the peak fitting for the high resolution XPS measurements[a,b]

Sample	Si 2p	Sr 3d 5/2	Sr 3d 3/2	ΔSr 3d	C 1s	Ti 2p 1/2	Ti 2p 3/2	Δ Ti 2p	O 1s[c]	O1s[c]
Ref. STO(001)		132.5 (0.9)	134.3 (0.9)	1.8	285.0 (1.8)	459.0 (1.0)	464.7 (1.1)	5.7	530.0 (0.8)	531.4 (2.2)
OTS/STO(001)	102.5 (1.3)	132.5 (0.9)	134.2 (1.0)	1.7	285.0 (1.2)	459.0 (1.1)	464.7 (1.2)	5.7	530.2 (0.8)	531.8 (2.4)
OTS/STO:Nb(001)	102.6 (1.4)				285.0 (1.2)	459.2 (1.2)	464.7 (1.9)	5.5	530.2 (0.8)	531.7 (2.5)
DTS/STO(001)	102.5 (1.3)	132.4 (1.0)	134.2 (1.0)	1.8	285.0 (1.3)	459.0 (1.1)	464.6 (1.4)	5.6	530.1 (0.8)	531.4 (2.2)

[a]Referenced to C1s @ 285.0eV, FWHM of fits are indicated between parentheses
[b]Δ is the splitting between the two Ti peaks or two Sr peaks
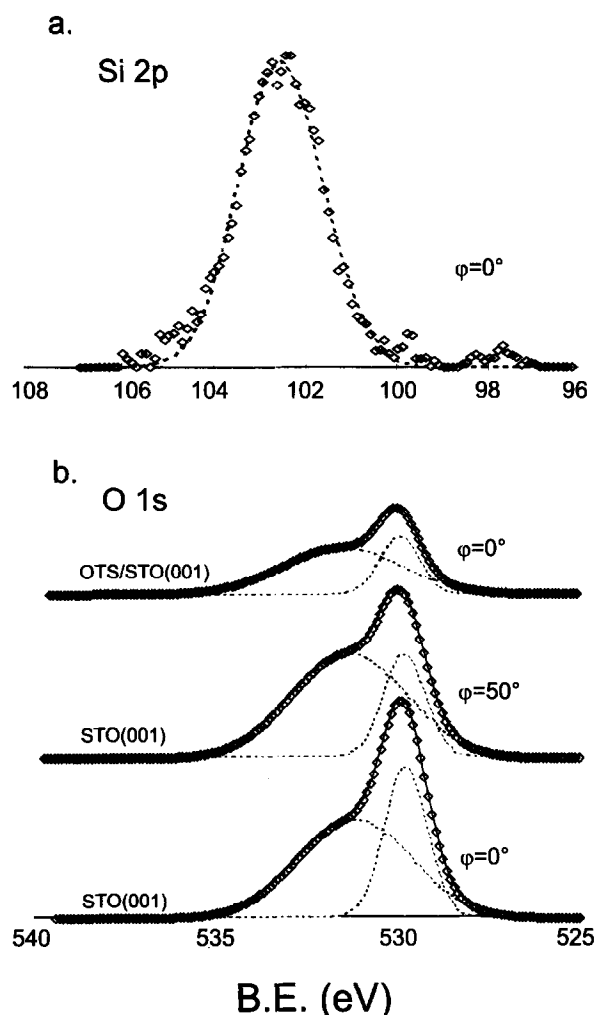[c]O1s is fitted as two singlets

Figure 2 High resolution XPS spectra of (a) the Si 2p region for a monolayer of OTS on STO(001) and (b) the O 1s region at $\varphi = 0°$ and $\varphi = 50°$ of an unmodified STO(001) substrate and of a monolayer of OTS on a STO(001) substrate (at $\varphi = 0°$)

agree well with the ellipsometry thickness determination for the same films.

RAIRS

In *Figure 3*, the results for the C–H stretching region $(2700–3100 \text{cm}^{-1})$ is presented for a monolayer of OTS on STO(001) and STO(110). The other two substrates [i.e. STO(103) and STO:Nb(001)] are not included since these two spectra are intrinsically more difficult to interpret because of the dielectric function of the substrate[13,14]. In the shown spectra, the CH_2 stretching modes at ~2850 and ~2917cm^{-1} are clearly visible (see *Table 3*). The positions of the peaks indicate the presence of a crystalline environment for the alkane chain[7,8b,15]. The apparent absence of the methyl vibrations at 2870 and 2962cm^{-1} is due to the optical nature of the substrate and not to the lack of any order at the chain ends[14,15]. Opposite to metals (with high absorption), the electric field on the surface of oxidic substrates also has a parallel component that can result in an increase in reflectivity and conse-
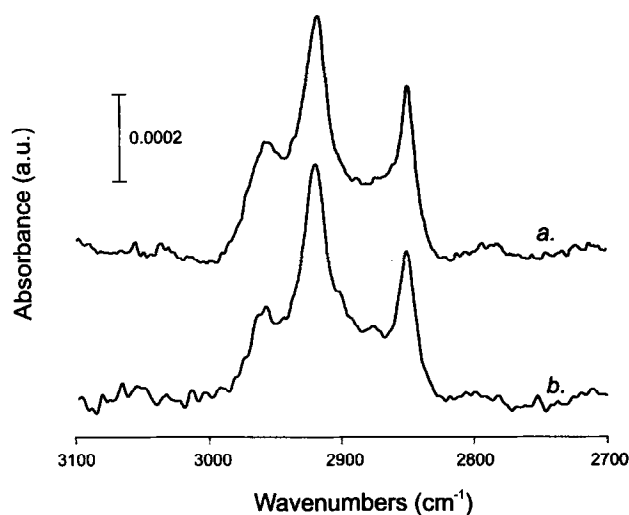

Figure 3 Reflective absorption infrared spectra of (a) a monolayer of OTS on a SrTiO₃(110) substrate and (b) a monolayer of OTS on a SrTiO₃(001) substrate

Table 3 Assignment of vibrational modes of alkyl chains[a]

Mode assignment[b]	Approximate peak frequencies (cm^{-1})		
	Bulk crystalline alkane[a]	Liquid alkane[a]	OTS-STO
CH3, asym., str., op (ra)	2962		
CH3, asym., str., ip (rb)	2952	~2957	~2956
CH2, asym., str., (d−)	2915	2928	2917
CH3, sym., str., (r+)	2870		
CH2, sym., str., (d+)	2846	2856	2850

[a]Based on data reported previously for hexadecane and octadecane polycrystalline material[17]
[b]Abbreviations: asym. = asymmetric, sym. = symmetric, str. = stretch, op = out of plane, ip = in plane

quently in negative absorption peaks. The resulting complex absorption spectrum is the superposition of vibrational modes both perpendicular and parallel to the interface (positive and negative absorption peaks, respectively) and, therefore, certain expected peaks are cancelled out. However, peak intensities of the CH_2 stretching modes are comparable to the intensities of OTS on the native oxide of silicon[7,15]. The methyl antisymmetric C–H stretching peak at 2956cm^{-1} is also observed in infrared transmission spectra of OTS on SiO₂[7,15a].

The fact that there are only small differences in the spectra for the (001) and (110) faces of STO indicates that films of comparable quality can be formed. A geometric argument on the packing of OTS molecules, based on the position of hydroxyl groups on the surface, can be made. Assuming that the hydroxyl species are bonded exclusively to either Sr or Ti and each alkyl chain is bonded to one hydroxyl, each chain would occupy an area of ~15Å^2 on (001) surfaces. On (110) surfaces, on the other hand, an area of ~21Å^2 per chain is available, which closely resembles the optimum area for an alkyl chain[1]. These data, there-

fore, indicate formation of not only a few anchoring bonds (i.e. Si–O–(Ti,Sr) bonds), but considerable cross-linking between neighbouring chains, since the films under investigation are stable up to 150°C. Furthermore, no differences are found for monolayers of OTS on as-cleaned and annealed STO(001) substrates. It is thus likely that the quality of the monolayer does not depend on the surface termination of the substrate.

Films that were adsorbed on STO at temperatures larger than approximately 25°C show a more liquid-like behaviour with the CH_2 stretching modes located at 2853 and 2923cm^{-1}, respectively. Only lately has the temperature during adsorption been recognized as an important parameter in the self-assembly of alkyltrichlorosilanes[4]. In several reports[4,7], it has been found that a critical temperature T_c exists, above which no dense high quality films can be formed. Our observation that films of lower quality (less order and less densely packed, as judged by ellipsometry) are formed if the temperature of the adsorption solution is above approximately 25°C is in good agreement with the range given by Parikh *et al.*[7] (24±4°C) for the formation of OTS monolayers on SiO_2. The temperature dependence of, e.g., the position of the stretching modes and the thickness of the OTS monolayer on STO is not studied in more detail, but we have found that an adsorption temperature of approximately 20°C yields highly ordered and densely packed monolayers.

SE

The usual procedure to determine the thickness of an overlayer on a substrate is to obtain a reference spectrum of the substrate (or of a multiple stack of layers on a substrate), followed by the measurement of the film on the same or an equivalent substrate. The usual problem in ellipsometric studies is to relate the two measured quantities to three unknown variables of the overlayer (the complex dielectric function and the thickness d of the overlayer). In the case of simple alkyl chains, one can assume that the refractive index is constant over the complete energy range and is equal to 1.45[8a], and that the absorption of the hydrocarbon chain can be neglected. Concluding, the two measured parameters should be sufficient to determine the thickness of the monolayer in this case.

The most straightforward procedure to analyze the data is to calculate an (pseudo-) optical function for the substrate from its spectrum. Using this optical function, one can calculate the response of a (monolayer) film as a function of thickness, using an isotropic and homogeneous three-layer structure. By comparison with the measured spectrum, linear regression analysis is used to minimize the unbiased estimator of a least-square deviation to find the

optimum thickness for each energy. The accuracy of the individual fits can be estimated by calculating the 90% confidence limits[16]. To obtain the best overall fit, we have calculated an error function σ_{tot} (defined as $\sum_E \delta(\Delta)^2 + \delta(\Psi)^2$, with $\delta\Delta = \Delta_{calc} - \Delta_{meas}$ and $\delta\Psi = \Psi_{calc} - \Psi_{meas}$) over all energies, using the previously found thicknesses. Furthermore, to estimate errors in alignment, the system is aligned several times and the measured Δ and Ψ for each of the independent measurements are compared to each other. It is found that typical alignment errors for Δ and Ψ are smaller than 0.5°, resulting in relatively small thickness variations.

In *Figure 4*, the calculated thickness, as a function of the energy, is shown for a single monolayer of OTS on STO (♦) and a lamellar structure of OTS on STO:Nb(001). The ellipsometry measurements shown are done on the same films for which the topography is shown in *Figure 1*. The error bars shown are calculated according to the 90% confidence limits. In the inset, σ_{tot} for both films is shown for all independent determined thicknesses. Below 1.7 and above 4.0eV, the errors in thickness are large due to the low reflectance at these energies, and around 3.0eV the angle of incidence is aligned to be Brewster's angle, where small errors in δ result in large errors in the thickness. For the first film, an overall minimum in σ_{tot} is present at 2.43nm, which we will assume to be the thickness of the monolayer[8a], whereas the second film displays a larger thickness ($d = 4.55$nm), due to extra bilayers (■). Between 1.7 and 4.0eV, a relatively uniform thickness is found for both samples, with very small errors per energy. Decreased thicknesses were found for films that were rubbed to remove the
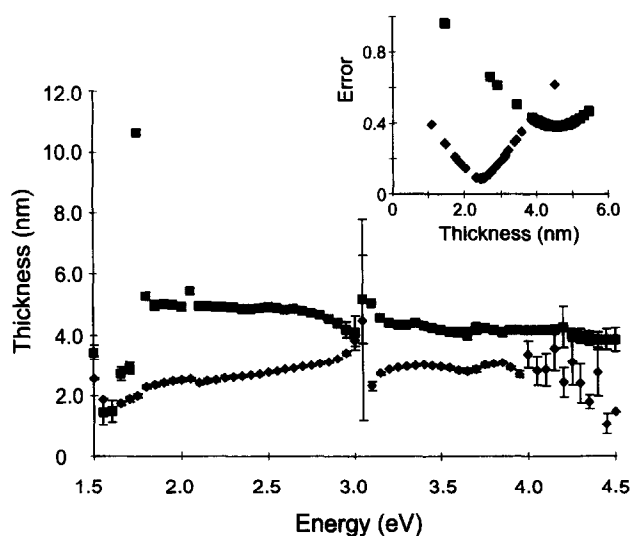

Figure 4 Calculated thickness as function of the energy of a monolayer of OTS on a SrTiO₃(001) surface (♦) and the lamellar structures of OTS on SrTiO₃:Nb(001) (■). In the inset, the summed error σ_{tot} over all energies as function of the thickness is shown for both fits. It is assumed that the minimum in the curve yields the thickness of the monolayer. The topography of the films used are shown in *Figures 1a* and *b*, respectively

adventitious lamellae ($d = 2.2-2.4$ nm), which indicates the growth of less densely packed monolayers.

CONCLUSION

We have studied the formation of alkylsiloxane monolayers on different faces of SrTiO$_3$ substrates and characterized the resulting layers by AFM, wettability, ARXPS, RAIRS and SE. Densely packed, highly ordered monolayers are formed if the temperature during adsorption is controlled below a critical temperature (approximately 25°C), and if high humidity ($> 50\%$) is avoided. Few differences in coverage, chain environment and final thicknesses exist between SrTiO$_3$(001), (110) and Nb-doped SrTiO$_3$(001), although these substrates have different terminating planes. This is an indication that there is no commensurate overlayer on all surfaces, as is the case for the thiols on gold. An intrinsically rough substrate such as SrTiO$_3$(103) yields monolayers with somewhat lower quality, but still yields reasonably packed layers.

ACKNOWLEDGEMENTS

REFERENCES

1. Ulman, A., *An Introduction to Ultrathin Organic Films, from Langmuir–Blodgett to Self-Assembly*. Academic, 1991.

2. (a) Carson, G. and Granick, S. J., *J. Appl. Polym. Sci.*, 1989, **37**, 2767; (b) Maoz, R. and Sagiv, J., *J. Colloid and Interf. Sci.*, 1984, **100**, 465; (c) Allara, D. L., Parikh, A. N. and Rondelez, F., *Langmuir*, 1995, **11**, 2357.

3. (a) Blank, D. H. A., Adelerhof, D. J., Flokstra, J. and Rogalla, H., *Physica C*, 1990, **167**, 423; (b) Henrich, V. E. and Cox, P. A., *The Surface Science of Metal Oxides*, Cambridge University Press, 1994.

4. (a) Brzoska, J. B., Shahidzadeh, N. and Rondelez, F., *Nature*, 1992, **360**, 719; (b) Brzoska, J. B., Ben Azouz, I. and Rondelez, F., *Langmuir*, 1994, **10**, 4367.

5. Kawasaki, M., Takahashi, K., Maeda, T., Tsuchiya, R., Shinohara, M., Ishiyama, O., Yonezawa, T., Yoshimoto, M. and Koinuma, H., *Science*, 1994, **266**, 1540.

6. Bain, C. D., Troughton, E. B., Tao, Y.-T., Evall, J., Whitesides, G. M. and Nuzzo, R. G., *J. Am. Chem. Soc.*, 1989, **111**, 321.

7. Parikh, A. N., Allara, D. L., Ben Azouz, I. and Rondelez, F., *J. Phys. Chem.*, 1994, **98**, 7577.

8. (a) Wasserman, S. R., Tao, Y.-T. and Whitesides, G. M., *Langmuir*, 1989, **5**, 1074; (b) Offord, D. A. and Griffin, J. H., *Langmuir*, 1993, **9**, 3015; (c) McGovern, M. E., Kallury, K. M. R. and Thompson, M., *Langmuir*, 1994, **10**, 3607.

9. (a) Nagarkar, P. V., Searson, P. C. and Gealy III, F. D., *J. Appl. Phys.*, 1991, **69**, 459; (b) Kawai, J., Tamura, K., Owari, M. and Nikei, Y., *J. Electron. Spectrosc. Relat. Phenom.*, 1992, **61**, 103; (c) Gonda, S., *Physica C*, 1993, **216**(112), 160; (d) Pilleaux, M. E., Grahmann, C. R. and Fuenzalida, V. M., *J. Am. Ceram. Soc.*, 1994, **77**, 1601.

10. Alfonsetti, R., de Simone, G., Lozzi, L., Passacantado, M., Picozzi, P. and Santucci, S., *Surf. Interface Analysis*, 1994, **22**, 93.

11. Aarnink, W. A. M., Gao, J., Rogalla, H. and van Silfhout, A., *Appl. Surf. Sci.*, 1992, **55**, 117.

12. Laibinis, P. E., Bain, C. D. and Whitesides, G. M., *J. Phys. Chem.*, 1991, **95**, 701.

13. (a) Parikh, A. N. and Allara, D. L., *J. Phys. Chem.*, 1992, **92**, 927; (b) Mielczarski, J. A., *J. Phys. Chem.*, 1993, **97**, 2649.

14. Kropman, B. L., Blank, D. H. A. and Rogalla, H., in preparation.

15. (a) Allara, D. L., Parikh, A. N. and Rondelez, F., *Langmuir*, 1995, **11**, 2357; (b) Hoffmann, H., Mayer, U., Brunner, H. and Krischanitz, A., *Vib. Spectrosc.*, 1995, **8**, 151.

16. (a) Collins, R. W., Allara, D. L., Kim, Y.-Y., Lu, Y. and Shi, J., in *Characterisation of Organic Thin Films*, ed. A. Ulman, Butterworth, 1995; (b) Shi, J., Hong, B., Parikh, A. N., Collins, R. W. and Allara, D. L., *Chem. Phys. Lett.*, 1995, **246**, 90.

17. Snyder, R. G., *Macromolecules*, 1990, **23**, 2081.